Annexin II/Annexin II Receptor Axis Regulates Adhesion, Migration, Homing, and Growth of Prostate Cancer

Yusuke Shiozawa,[1] Aaron M. Havens,[1,2] Younghun Jung,[1] Anne M. Ziegler,[1] Elisabeth A. Pedersen,[1] Jingcheng Wang,[1] Jianhua Wang,[1] Ganwei Lu,[3] G. David Roodman,[3] Robert D. Loberg,[4] Kenneth J. Pienta,[4] and Russell S. Taichman[1]*

[1]Department of Periodontics and Oral Medicine, University of Michigan School of Dentistry, Ann Arbor, Michigan

[2]Harvard School of Dental Medicine, Boston, Massachusetts

[3]Medicine-Hematology/Oncology, University of Pittsburgh, Pittsburgh, Pennsylvania

[4]Department of Internal Medicine, Division of Hemotology/Oncology, University of Michigan School of Medicine, Ann Arbor, Michigan

ABSTRACT

One of the most life-threatening complications of prostate cancer is skeletal metastasis. In order to develop treatment for metastasis, it is important to understand its molecular mechanisms. Our work in this field has drawn parallels between hematopoietic stem cell and prostate cancer homing to the marrow. Our recent work demonstrated that annexin II expressed by osteoblasts and endothelial cells plays a critical role in niche selection. In this study, we demonstrate that annexin II and its receptor play a crucial role in establishing metastasis of prostate cancer. Prostate cancer cell lines migrate toward annexin II and the adhesion of prostate cancer to osteoblasts and endothelial cells was inhibited by annexin II. By blocking annexin II or its receptor in animal models, short-term and long-term localization of prostate cancers are limited. Annexin II may also facilitate the growth of prostate cancer in vitro and in vivo by the MAPK pathway. These data strongly suggest that annexin II and its receptor axis plays a central role in prostate cancer metastasis, and that prostate cancer utilize the hematopoietic stem cell homing mechanisms to gain access to the niche. J. Cell. Biochem. 105: 370–380, 2008.   © 2008 Wiley-Liss, Inc.

KEY WORDS: ANNEXIN II; ANNEXIN II RECEPTOR; PROSTATE CANCER; METASTASIS; NICHE

Cancer of the prostate gland (PCa), as well as those arising in many other tissues, displays a remarkable propensity to invade and survive in bone. Nearly 10% of patients present with bone metastasis, and almost all patients who die of PCa have skeletal involvement [Coleman, 2006]. Therefore, identifying the molecular mechanisms that regulate osseous metastasis is of clinical importance so as to determine those individuals at greatest risk for the development of metastasis. This research may also help design therapeutics aimed at decreasing metastatic risk or their complications.

The metastatic process is functionally similar to the migrational or "homing" behavior of hematopoietic stem cells (HSC) to the bone marrow. Numerous molecules have been implicated in regulating HSC homing, participating as both chemoattractants and regulators of cell growth. Our previous work has drawn heavily on the parallels between HSC homing and the homing of PCa cells to the marrow. As a result, we identified that PCa cells use the CXC chemokine CXCL12 or SDF-1 and its receptors CXCR4 [Taichman et al., 2002; Sun et al., 2003, 2005; Wang et al., 2005] and CXCR7/RDC1 [Wang et al., 2008] as key elements in metastasis and growth in bone.

Identification of the HSC niche in the marrow is an active area of investigation [Calvi et al., 2003; Zhang et al., 2003; Arai et al., 2004; Kiel et al., 2005; Taichman, 2005]. One protein in high abundance in the marrow is annexin II (Anxa2) (or p36, calpactin I heavy chain, and lipocortin II [Raynal and Pollard, 1994]). Anxa2 is a 36 kDa peripheral membrane protein expressed by endothelial cells, early myeloid cells, some tumor cells [Menell et al., 1999; Brownstein et al., 2001; Falcone et al., 2001], and osteoblasts [Takahashi et al., 1994; Wang and Kirsch, 2002; Jung et al., 2007]. Anxa2 exists as a monomer, a heterodimer, or a heterotetramer [Gerke and Weber,

1984; Glenney, 1986]. Anxa2 tetramer is composed of two copies of a 36 kDa heavy chain (Anxa2 or p36), and two 11 kDa light chains (p11) [Gerke and Weber, 1984]. The protein itself has two structural domains; an amino-terminal domain, which includes the first 30 amino acids of the p36 heavy chain, the serine and tyrosine phosphorylation sites and sites for binding the p11 light chain [Glenney, 1986]. The formation of the heterotetramer permits binding to the plasma membrane [Thiel et al., 1992]. The expression of Anxa2 is known to be regulated by insulin, fibroblast growth factor (FGF), and epidermal growth factor (EGF) [Zhao et al., 2003]. Enhanced Anxa2 expression has also been reported in human hepatocellular carcinoma, pancreatic adenocarcinoma, high-grade glioma, gastric carcinoma, and acute promyelocytic leukemia [Diaz et al., 2004]. Anxa2 is known to interact with a number of extracellular matrix molecules such as tenascin-C and proteolytic enzymes including tissue plasminogen activator (t-PA) and cathepsin B [Chung and Erickson, 1994; Fitzpatrick et al., 2000; Mai et al., 2000]. Accordingly, Anxa2 may participate in plasminogen activation, cell adhesion, and tumor metastasis and invasion.

Based upon its distribution in marrow, Anxa2 is likely to play several roles in regulating hematopoiesis. On endothelium, Anxa2 regulates the plasmin/plasminogen activator system and may play a role in fibrinolytic surveillance by anchoring key components of the fibrinolytic cascade [Brownstein et al., 2001; Falcone et al., 2001]. Anxa2 is known to serve as a binding site for beta 2-glycoprotein I, a phospholipid-binding protein from plasma [Baran et al., 2000]. Other ligands include a vitamin D analog that is inhibited in rat osteoblasts by Ca^{2+} [Baran et al., 2000]. In bone, Anxa2 has been demonstrated to play a role in osteoclastic activation and osteoblast mineralization, although the mechanisms for these actions remain unclear [Takahashi et al., 1994; Wang and Kirsch, 2002]. One scenario is that extracellular Anxa2 levels are regulated by 1,25-dihydroxyvitamin D3 that stimulates the proliferation of osteo-clastic precursors possibly through T-cell intermediaries to secrete granulocyte-macrophage colony stimulating factor (GM-CSF) [Menaa et al., 1999].

Our recent work in this field has demonstrated that Anxa2 expressed by osteoblasts and endothelial cells plays a critical role in niche selection [Jung et al., 2007]. We have demonstrated that the engraftment of HSCs and survival of lethally irradiated animals during experimental bone marrow transplantation are sharply curtailed in the presence of neutralizing Anxa2 antibodies, and N-terminal Anxa2 peptides [Jung et al., 2007]. Moreover, fewer HSCs are found in the marrows of *Anxa2*-deficient animals. Among the most compelling mechanisms to account for these observations is that Anxa2 acts as an adhesion ligand for HSCs homing [Jung et al., 2007].

In this study, we draw parallels between PCa metastasis and HSC homing to the niche. Anxa2 itself is associated with proliferating and invasive cancers, possibly as a marker of malignancy [Reeves et al., 1992] including lung, pancreatic, brain, colon, and gastric carcinomas, and is correlated with poor prognosis [Cole et al., 1992; Vishwanatha et al., 1993; Roseman et al., 1994; Emoto et al., 2001; Diaz et al., 2004]. Yet, the loss of Anxa2 expression appears to be specific for PCa disease [Chetcuti et al.,

2001; Banerjee et al., 2003; Kirshner et al., 2003; Liu et al., 2003; Smitherman et al., 2004; Semov et al., 2005]. Our finding indicates that Anxa2 serves as an adhesion molecule for PCa, and blocking Anxa2 or its receptor limits metastasis in animal models. Anxa2 may also facilitate the growth of PCa in vitro and in vivo via partially through activation of the MAPK pathway. Taken together, these data strongly suggest that annexin II plays a central role in PCa metastasis, and that PCa utilize HSC homing mechanisms to gain access to the niche.

MATERIALS AND METHODS

CELL CULTURE
PC-3 (CRL-1435), DU145 (HTB-81), and LNCaP (CRL-1740) prostate cancer cell lines were obtained from the American Type Culture Collection (Rockville, MD). The metastatic subline LNCaP C4-2B were originally isolated from a lymph node of a patient with disseminated bony and lymph node involvement [Wu et al., 1998]. PC-3[Luc] cells were constructed by stably transfecting PC-3 cells with luciferase construct, as previously described [Loberg et al., 2006]. The human bone marrow endothelial cells (HBMECs) were isolated from a normal Caucasian male and immortalized with SV40 large T-antigen [Lehr and Pienta, 1998]. Cells were cultured in RPMI 1640 (Invitrogen, Carlsbad, CA) and were supplemented with 10% fetal bovine serum (FBS; Invitrogen) and 1% penicillin-streptomycin (Invitrogen), and maintained at 37°C, 5% CO_2, and 100% humidity.

Anxa2 RECEPTOR (Anxa2r) SILENCING
A 60-bp oligonucleotide, containing 19-nucleotides to a portion of the human Anxa2r and its reverse complement sequences separated by a 9-nucleotide spacer sequence, were subcloned into the BglII and HindIII restriction sites of the 3.2-kb plasmid pSUPER containing the H1-RNA promoter (Oligoengine, Seattle, WA). PC-3[Luc] cells were transfected with siRNA Anxa2r vectors (PC-3[siAnxa2r] cells) and a scrambled control (PC-3[siControl] cells) using Superfect (QIAGEN, Valencia, CA) as described previously [Jung et al., 2007]. siRNA knock down was monitored by real-time reverse transcrip-tion-polymerase chain reaction (QPCR).

HUMAN OSTEOBLASTS
Human osteoblasts were established by explant culture from normal human trabecular bone obtained from patients undergoing orthopedic surgery in accordance with the University of Michigan's Investigational Review Board, as previously described [Taichman and Emerson, 1994].

ISOLATION OF PRIMARY MURINE CALVARIAL CELLS
Primary calvarial cells were isolated, as previously described [Koh et al., 2005]. Briefly, calvariae of mice (1- to 4-day-old) were dissected, isolated from periosteum, and subjected to sequential digestions of 20, 40, and 90 min in collagenase A (2 mg/ml; Roche Molecular Biochemicals, Indianapolis, IN) with 0.25% trypsin (Invitrogen). Cells from the third digestion were plated in α-MEM (Invitrogen) with 10% FBS and 1% penicillin and streptomycin.

MURINE MODELS

All experimental procedures were approved by the University of Michigan Committee for the Use and Care of Animals (UCUCA). C57BL6 mice, male severe combined immune deficient (SCID) mice (5–6 weeks of age), and male athymic (nude) mice (4–6 weeks of age) were purchased from Harlan Bioscience (Indianapolis, IN). The laboratory of Dr K.A. Hajjar (Weill Medical College of Cornell University, New York, NY) generated the $Anxa2$-deficient ($Anxa2^{-/-}$) animals used in our study and graciously provided our laboratory with a pair of the homozygous $Anxa2^{-/-}$ mice for breeding.

ANTIBODIES AND REAGENTS

The anti-Anxa2 antibody (Clone 5; mouse IgG1) was purchased from BD Pharmingen (San Diego, CA). Antibodies targeting Anxa2r were generated in the laboratory of Dr. G.D. Roodman (University of Pittsburgh, Pittsburgh, PA) and were described in detail previously [Lu et al., 2006]. The antibodies to phosphorylated Akt (Ser473), total Akt, phosphorylated p44/42 MAP kinase (Thr202/Tyr204), total p44/42 MAP kinase, and horseradish peroxidase (HRP)-labeled goat anti-rabbit IgG (H + L) were obtained from Cell Signaling Technology (Danvers, MA). The control antibodies for these investigations included immonoglobulin Ig G1κ (clone MOPC 31C; Sigma–Aldrich, St. Louis, MO), IgG1 (clone X40; Becton-Dickinson, San Jose, CA), IgG2a (clone 20102; R&D Systems, Minneapolis, MN). Purified bovine lung Anxa2 was purchased from Biodesign International (Saco, ME). Anxa2 N-terminal peptide corresponding to the 1–12 amino acids and a random peptide (TVLLHEICKSSL) were synthesized, as previously detailed [Jung et al., 2007]. Recombinant human CXCL12 was purchased from R&D Systems.

IMMUNOHISTOCHEMISTRY

Murine bones were harvested and fixed in 10% buffered formalin and decalcified in EDTA, and 2–3 μM paraffin-embedded slides were prepared and stained with antibody to Anxa2 or an IgG matched isotype control in conjunction with a HRP-AEC staining system kit using anti-mouse biotinylated antibodies following the manufactures protocols (R&D Systems).

Human osteoblasts were cultured in Lab-Tek II 4-chamber slides (Nalge Nunc International, Naperville, IL) at 5×10^4 cells/chamber. After 24 h, fixed in 4% paraformaldehyde for 25 min at room temperature, washed and endogenous peroxidase activity quenched with 75 mM NH4Cl and 20 mM Glycine in PBS at room temperature for 10 min. Thereafter, primary antibody incubations at a 1:200 dilution in PBS using the anti-Anxa2 or an IgG matched isotype control for 1 h at room temperature. Antibody detection was performed using an HRP-AEC staining kit (R&D Systems), and counter stained with hematoxylin (Sigma–Aldrich).

BINDING ASSAYS

Anxa2 binding assays were performed with purified bovine lung Anxa2 or Bovine Serum Albumin (BSA; Sigma–Aldrich) plated into 96-well plates for 24 h at 4°C, washed, and then blocked with 0.1% BSA for 2 h.

For cell-to-cell binding assays, the human osteoblasts, murine calvarial cells, and HBMECs were plated onto 96-well plates at a concentration of 10,000 cells per well (100 μl per well) in growth mediums, and the cultures were incubated for 2 days.

PC-3, PC-3^{siAnxa2r}, or PC-3^{siControl} cells were labeled with 2.5 μg/ml of the lipophilic dye carboxyfluorescein diacetate (CFDA; Molecular Probes, Eugene, OR) in RPMI for 30 min at 37°C, and washed in PBS. Thereafter, the cells were left for 30 min to reduce nonspecific background, and subsequently resuspended in PBS to deliver 10^5 cells/well in the adhesion assay. Adhesion assays were performed in PBS containing Ca^{+2}/Mg^{+2} where the cells were added to a final reaction volume of 100 μl at 4°C. After washing fluorescence was quantified. In some cases, the cells were incubated in 5 μg/ml of an anti-Anxa2 or IgG matched isotype control antibody, or 1 μg/ml of an Anxa2 N-terminal peptide or a random peptide control to block adhesion for 15 min on ice prior to seeding onto the monolayers.

TRANSWELL CHEMOTAXIS ASSAYS

Cell invasion into a reconstituted extracellular matrices coating of Matrigel^{TM} overlaid on 8 μM pore sized in polyethylene terephthalate membranes was performed in dual chambered invasion plates (BD Biosciences, San Jose, CA) as previously described [Sun et al., 2007; Wang et al., 2008]. Spontaneous invasion was compared to invasion supported by Anxa2. For blocking studies, rhCXCL12 at a final concentration of 200 ng/ml was added to the lower chamber, and Anxa2 N-terminal peptide or a random peptide control at a final concentration of 1 μg/ml was added to the upper chamber along with the cells.

REVERSE TRANSCRIPTION–PCR (RT–PCR) AND QPCR

RT-PCR and QPCR was carried out using standard techniques. Briefly, total RNA was isolated using RNeasy Mini Kit (QIAGEN), and first-strand cDNA was synthesized in a 20 μl reaction volume using 0.4 μg of total RNA. The sequences of the forward and reverse primers of Anxa2r were 5′-CGGAGTCTACTGGCAAAACG-3′ and 5′-GCCTTCTGCTGCTATCTAAG-3′. The reaction profile was 94°C for 1 min, 60°C for 1 min, and 72°C for 2 min for 35 cycles, followed by a 10-min extension at 72°C. PCR products were separated by electrophoresis in 1.2% agarose gels and visualized by ethidium bromide staining.

RT products were analyzed by QPCR in TaqMan® Gene Expression Assays of several target genes: Anxa2r (Hs01588662_s1) and β-actin (Hs99999903_m1) (Applied Biosystems, Foster City, CA). QPCR analysis was performed using 15.0 μl of TaqMan® Universal PCR Master Mix (Applied Biosystems), 1.5 μl of TaqMan® Gene Expression Assay (forward and reverse primers at 18 μM and Taqman probe at 5 μM), 1 μl of the RT product, and 12.5 μl of RNAse/DNAse-free water in a total volume of 30 μl. Reactions without template and/or enzyme were used as negative controls. The 2nd step PCR reaction (95°C for 30 s, 60°C) was run for 40 cycles after an initial single cycle of 95°C for 15 min to activate the Taq polymerase. The PCR product was detected as an increase in fluorescence using an ABI PRISM 7700 instrument (Applied Biosystems). RNA quantity (C_R) was normalized to the housekeeping gene β-Actin control by using the formula $C_R = 2^{(40-Ct\text{ of sample})-(40-Ct\text{ of control})}$. The threshold cycle (Ct) is the cycle at which a significant increase in fluorescence occurs.

TISSUE MICROARRAY AND IMMUNOSTAINING

Human prostate adenocarcinoma tissue microarray was purchased from US Biomax, Inc. (Rockville, MD). Tumors were graded using the Gleason grading system and examined to identify areas of benign prostate, prostate cancer and bone metastasis. The formalin-fixed, paraffin-embedded tissues were deparaffinized and placed in a pressure cooker containing 0.01 M buffered sodium citrate solution (pH 6.0), boiled and chilled to room temp for antigen retrieval. The slides were incubated overnight at room temperature with anti-Anxa2r antibody diluted 1:100. A blinded pathologist analyzed arrays and staining intensity was ranked on a scale from 0 to 3 (0, negative; 1, weak; 2, moderate; and 3, strong intensity staining).

Anxa2 TREATMENTS

PC-3 cells (1×10^6) were cultured in six-well plates in RPMI medium (1 ml) without FBS for 5 h. After serum starvation, the cells were treated with 1,000 ng/ml Anxa2 for 5, 15, 30, 45, and 60 min. The cells were extracted for protein and analyzed for phosphorylated p44/42 MAP kinase (Thr202/Tyr204) and for phosphorylated Akt by Western blotting analysis. Total p44/42 MAP kinase and Akt were used as an internal control for loading.

PROLIFERATION ASSAYS

The murine calvarial cells from $Anxa2^{+/+}$ or $Anxa2^{-/-}$ mice were plated into triplicate 96-well plates at a concentration of 10,000 cells per well (100 μl per well) in growth medium with 0.1% FBS. The next day, PC-3^{Luc} cells were added to the wells at a concentration of 5,000 cells per well. Thereafter, the cultures were incubated in an atmosphere of 5% CO_2 and 95% O_2 at 37°C for 3 days. Proliferation was determined by using a CCD IVIS system with a 50-mm lens (Xenogen Corp., Alameda, CA) and the results were analyzed using LivingImage software (Xenogen Corp.).

IN VIVO METASTASIS ASSAYS

PC-3^{Luc} cells were introduced into male SCID mice by intracardiac (i.c.) injections. Immediately prior, the recipient mice were inoculated by intraperitoneal (i.p.) injections with (i) anti-Anxa2 antibody, (ii) the Anxa2 N-terminal peptide, or (iii) a mixed IgG matched isotype control antibodies/random peptide control each at 10 μg/kg. Short-term engraftment was assessed at 12 h by QPCR using for *luciferase 2CP* gene [*luc2CP*, CGGCTGGCAGAAGCTAT-GAA (forward), TCGCTGCACACCACGAT (reverse), and 5′-FAM-CTATGGGCTGAATACAAACC (TaqMan probe; Applied Biosystems)]. Data were normalized to mouse tissue β-actin (mm00607939-s1).

PC-3^{siAnxa2r} or PC-3^{siControl} cells were used to assess the role of Anxa2 in long-term PCa homing.

BIOLUMINESCENT IMAGING (BLI)

BLI was done as previously described through The University of Michigan Small Animal Imaging Resource facility [Loberg et al., 2007]. Briefly, cells were introduced into male SCID mice by i.c. injections. Mice were imaged at 30 days by BLI. Mice were injected with luciferin (40 mg/ml) by i.p. injections and ventral images were acquired 15 min postinjection under 1.75% isofluorane/air anesthesia. Total tumor burden of each animal was calculated using regions of interest (ROI) that encompassed the entire animal.

VERTEBRAL BODY TRANSPLANTS (VOSSICLES)

Lumbar vertebrae were isolated from $Anxa2^{+/+}$ or $Anxa2^{-/-}$ mice 7 days after birth. The vertebrae were sectioned into single vertebral bodies (vossicles). Athymic (nude) mice were used as transplant recipients. Four vossicles per mouse were implanted into sub-cutaneous (s.c.) pouches. Before implantations, PC-3^{Luc} cells were introduced into both vossicles (10,000 cells/10 μl of PBS). Mice were imaged at 30 days by BLI.

STATISTICAL ANALYSES

All in vitro experiments were performed at least three times with similar results and representative assay are shown. Numerical data are expressed as mean ± standard error. Statistical analysis was performed by ANOVA or Student's *t*-test using the GraphPad Instat statistical program (GraphPad Software, San Diego, CA) with significance at $P < 0.05$. For the QPCR assays, a Kruskal–Wallis test and Dunn's multiple comparisons tests were utilized with the level of significance set at $P < 0.05$.

RESULTS

Anxa2 IS EXPRESSED ON OSTEOBLASTS SURFACE IN BONE MARROW

To determine whether Anxa2 is expressed at the sites relevant to the localization of PCa to the bone marrow endosteal and endothelial niches, immunohistochemistry for Anxa2 was performed. As demonstrated in Figure 1A, Anxa2 immunoreactivity was most intense at the endosteal osteoblastic surfaces of the marrow closest the growth plate (Fig. 1A-1,2). In some cases, bone marrow endothelial cells also displayed immunoreactivity towards Anxa2 (Fig. 1A-1,3). No signal was observed in the absence of the specific anti-Anxa2 antibody (Fig. 1A-4) and the bone marrow from $Anxa2^{-/-}$ mice (Fig. 1A-5). Human primary osteoblasts also demonstrated perinuclear and cytoplasmic expression of Anxa2 in nearly all of the cells under basal conditions (Fig. 1B). These findings suggest that Anxa2 is expressed on osteoblasts in the bone marrow.

PCa BINDS AND MIGRATES TOWARDS Anxa2

Our recent studies demonstrate that HSCs use Anxa2 to bind to endothelial cells and osteoblasts [Jung et al., 2007]. Studies were therefore undertaken to determine if Anxa2 serves as an adhesive molecule for PCa. PC-3 cells bind to Anxa2 in a dose dependent manner (Fig. 2A-1), and other PCa cell lines not shown). Cell-to-cell adhesion assays were next performed using a bone marrow endothelial cells and osteoblasts that express abundant Anxa2. Here, the PCa cells bound rapidly to the HBMEC cells and the Anxa2 N-terminal competing peptide significantly reduced PC-3 cells binding to HBMECs compared to a scrambled control peptide (Fig. 2A-2). Next, we performed the binding assays between PC-3 cells and human or murine osteoblasts. The data demonstrate that the binding of PC-3 cells to human osteoblasts was significantly inhibited using antibody to Anxa2 (Fig. 2B-1). When the binding of PC-3 cells to osteoblasts derived from $Anxa2^{+/+}$ or $Anxa2^{-/-}$ mice was evaluated, it was noted that significantly more PC-3 cells bound
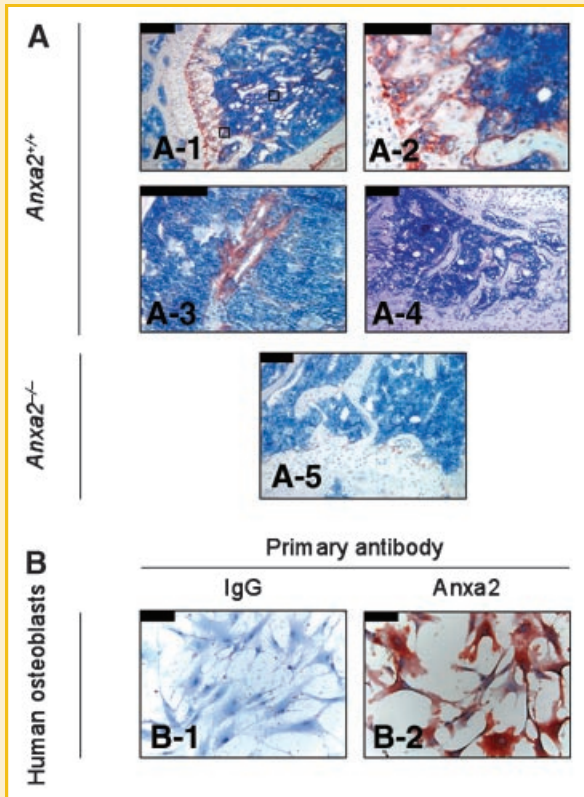
Fig. 1. Anxa2 protein is expressed in bone. A: Expression of Anxa2 protein in murine long bones. Mouse tibias were fixed in 10% formalin at 4°C before being decalcified in 10% EDTA (pH 7.4) and embedded in paraffin wax. Immunolocalization of Anxa2 protein was visualized using a monoclonal antibody (mAb) to Anxa2 or an IgG isotype matched control antibody. A-1: Anxa2-immunostained tibias (20× magnification). A-2: Higher magnification of (A-1) at 40× magnification and Anxa2 expression at the epiphyseal growth plates. A-3: Higher magnification of (A-1) at 40× magnification and Anxa2 expression at the bone marrow endothelial cells. A-4: IgG control (20× magnification). A-5: No Anxa2 expression in the tibia of $Anxa2^{-/-}$ animals (20× magnification). B: Expression of Anxa2 protein by primary human osteoblasts stained with anti-Anxa2 mAb or an IgG isotype matched control (20× magnification). B-1: IgG control immunoactivity on the human osteoblasts. B-2: Anxa2 expression on the human osteoblasts. Scale bars = 100 μm.

to the $Anxa2^{+/+}$ osteoblasts than to the $Anxa2^{-/-}$ osteoblasts (Fig. 2B-2).

Once tumor cells have adhered to and moved through the endothelium, they must invade through the extracellular matrix. The ability of Anxa2 to influence PCa invasion was studied using a reconstituted extracellular matrix in porous chambers. PC-3 cells were placed in the upper chamber in serum free medium, whereas Anxa2 at increasing doses was placed in the lower chamber to establish a chemoattractive gradient. After 8 h, quantification of the cells migrating into the reconstituted matrix in triplicate assays was performed. Anxa2 supported the invasion of PC-3 cells into the reconstituted matrix (Fig. 2C). To further determine if Anxa2 is used to localize PCa cells to tissue spaces, CXCL12 was employed to establish a chemoattractive gradient [Taichman et al., 2002]. When rhCXCL12 was placed in the bottom chamber, PC-3 cells migrated towards the chemokine (Fig. 2D). When Anxa2 was added to the

upper chamber of the culture dish with rhCXCL12 present in the bottom, fewer PC-3 cells migrated towards the chemokine CXCL12. Similar results were observed when an N-terminal competing Anxa2 peptide was included in the assay (Fig. 2D). These data support the notion that PCa binds to, and moves toward Anxa2, and further suggests that Anxa2 participates in tissue localization of PCa.

Anxa2 IS INVOLVED IN PCa METASTASIS

In order to test our hypothesis that Anxa2 is critical for the development of metastases in vivo, we established three experimental groups. In each case, the animals were inoculated with PC-3^{Luc} cells by *i.c.* injection. Immediately prior to the *i.c.* injection, the animals were injected *i.p.* with (i) an antibody to Anxa2, (ii) the N-terminal competing Anxa2 peptide, or (iii) an isotype matched, nonspecific antibody combined with a scrambled the amino acid sequence of the N-terminal competing peptide. The animals were subsequently sacrificed at 12 h and tissues were harvested. *Q*PCR was utilized as our primary outcome to detect the tagged human cells. As shown in Figure 3, all of the animals in injected with PC-3 cells alone demonstrated significant homing/lodging of the cancer cells in a number of tissues. Animals injected with antibody to Anxa2 and the Anxa2 N-terminal competing peptide significantly reduced the total metastatic load of the animals compared to the IgG/peptide treated control group. Animals not injected with human cells did not demonstrate any signal for luciferase (data not shown). These data suggested that Anxa2 plays an important role in short-term homing of PCa and regulates PCa metastasis.

Anxa2r EXPRESSED ON PCa

A single pass Anxa2r membrane receptor was cloned and identified to bind the p11 fraction of Anxa2 (Anxa2r) [Lu et al., 2006]. To determine if PCa cells express the Anxa2r, RT-PCR and *Q*PCR for the Anxa2r was performed. As demonstrated in Figure 4A, PC-3 cells expressed mRNA for the Anxa2r. We also performed *Q*PCR for 4 different human PCa cell lines to compare their expression levels. The Anxa2r mRNA was most strongly expressed by the DU145 cell line (Fig. 4B). Modest expression was seen in the PC-3, LNCaP, and C4-2B cell lines (Fig. 4B). Next, to evaluate the widest range of Anxa2r expression, PCa tissue microarrays were examined. Tumors were graded using the Gleason grading system and examined to identify areas of benign prostate and PCa. Staining of microarrays with antibody to Anxa2r revealed moderate-to-strong Anxa2r protein expression in clinically localized PCa samples with cytoplasmic and nuclear localization (Fig. 4C-1–6). Anxa2r protein expression was enhanced with increasing tumor grade, although statistically there were no significant differences in localized tumor and metastatic lesions (Fig. 4C-1–6, and data not presented).

Anxa2r INVOLVED IN PCa METASTASIS

To test whether Anxa2r is also critical for the development of metastases, siRNAs were employed to alter the expression of Anxa2r on PCa cells. PC-3^{Luc} cells were transfected with siRNAs targeting the Anxa2r. Our best siRNA was able to decrease Anxa2r mRNA expression by $\sim 60\%$ by 48h (Fig. 5A). By knocking down the Anxa2r, PCa cells bind less vigorously to HBMECs compared with
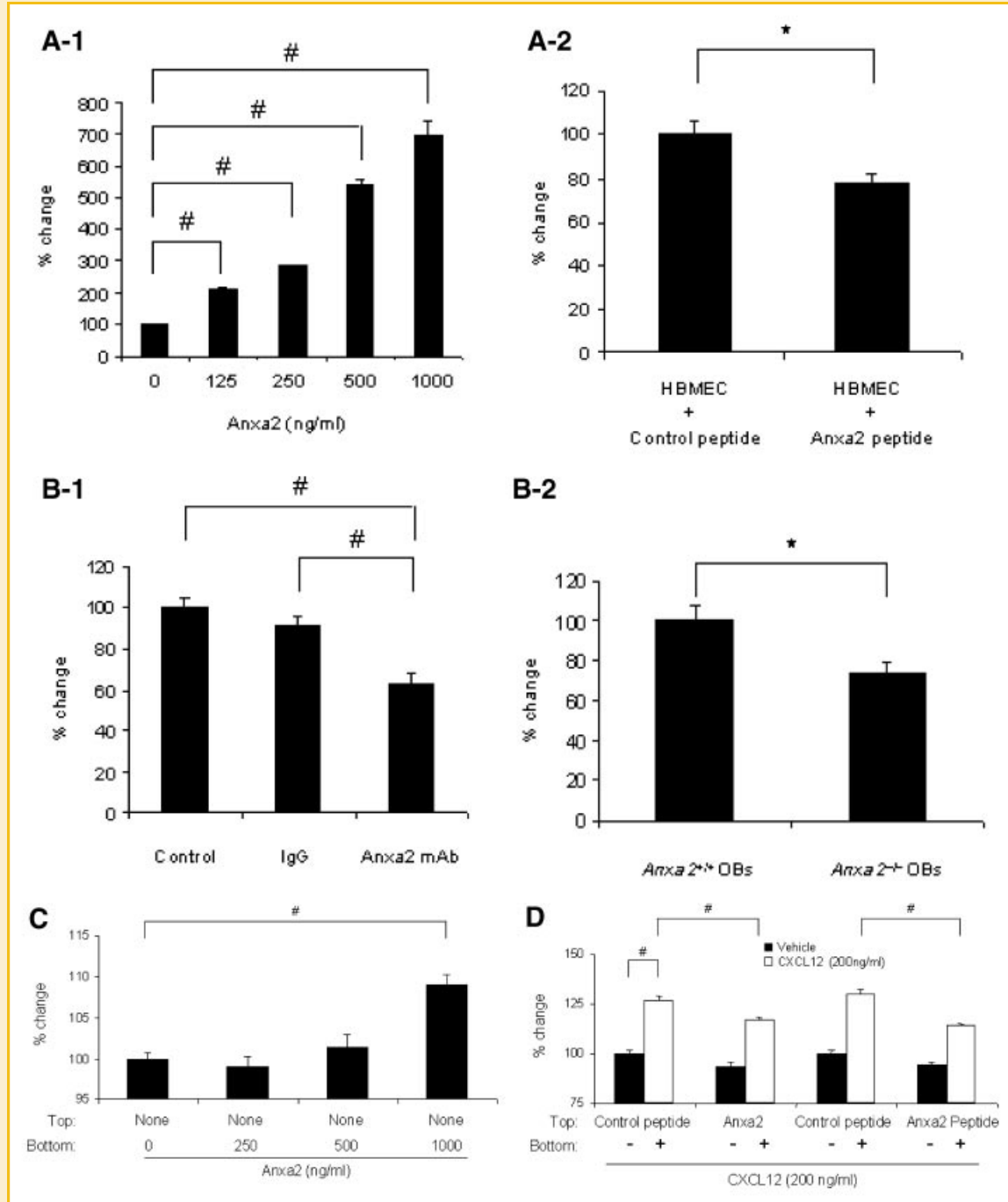
Fig. 2. Anxa2 regulates the adhesion of prostate cancer and prostate cancer invasion. A–1: Fluorescently labeled PC-3 cells were deposited directly into wells containing different concentrations (0–1,000 ng/ml) of purified bovine lung Anxa2 peptide and adhesion determined. A–2: PC-3 cells were layered on human bone marrow endothelial cells (HBMECs) in the presence of N-terminal Anxa2 peptide or a scramble control peptide. B–1: PC-3 cells were layered on human osteoblasts in the absence or presence of an anti-Anxa2 antibody or an isotype matched IgG control antibody (5 μg/ml). B–2: PC-3 cells were layered on wild-type murine osteoblasts ($Anxa2^{+/+}$ OBs) or $Anxa2^{-/-}$ murine osteoblasts ($Anxa2^{-/-}$ OBs). After 15 min incubation at 4°C, the non-adherent cells were removed. The number of adherent cells was quantified using a fluorescence plate reader. Data are presented as the mean ± standard error percentage of adherent cells from three independent experiments. $^*P < 0.05$ and $^#P < 0.01$ versus control by ANOVA. Invasion of PC3 cells into matrigel was used to evaluate the effects of Anxa2 on invasion. C: Matrigel invasion assays were performed with different concentrations of purified bovine lung Anxa2 peptide on PC-3 cell invasion. In (D), Matrigel invasion assays were used to evaluate the effect of neutralizing Anxa2 on the invasion of PC-3 cells in response to a chemotactic gradient established by CXCL12. Purified bovine lung Anxa2 or N-terminal Anxa2 or control peptides were seeded on the upper well of a Transwell chamber. The rhCXCL12 was added in the lower well (200 ng/ml). The results of at least three independent replicates are shown. $^#P < 0.01$ versus control by ANOVA.
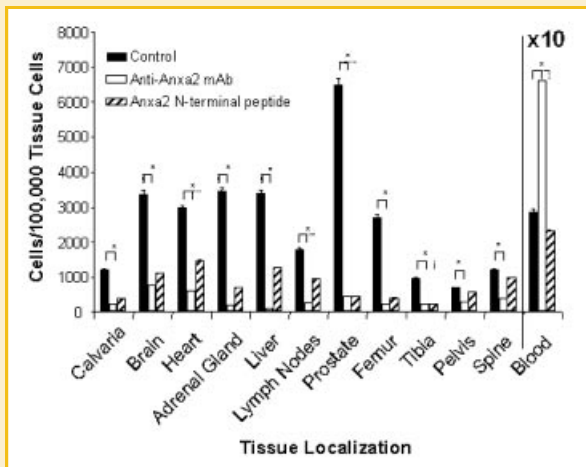
Fig. 3.   Anxa2 regulates short term homing of prostate cancer in vivo to bone. PC-3^{Luc} cells were administered by intracadiac injection into SCID mice in the presence of antibody to Anxa2, an N–terminal Anxa2 peptide, or mixed IgG matched isotype control antibodies and random peptide controls each at 10 μg/kg. The short–term homing capabilities of the prostate cancer were evaluated at 12 h. The level of engraftment was assessed by QPCR for luciferase and data were normalized to total mouse β–actin. Data are presented as the mean ± standard error (n = 5) where significance was determined using a Kruskal–Wallis test and Dunn's multiple comparisons with the level of significance set at $^*P < 0.05$.

Fig. 4.   Prostate cancer expresses Anxa2r. A: Representative conventional RT–PCR analysis of Anxa2r expression in PC–3 cell line. KG1a cells (acute myeloid leukemia cell line) served as positive controls for Anxa2r and H$_2$O served as negative controls. B: Representative QPCR analysis of Anxa2r in prostate cancer cell lines. Data are presented as the mean ± standard error from three independent PCR reactions. C: Representative elements of a tissue microarray in PCa stained with anti-Anxa2r antibody. C–1: Gleason grading 0. C–2: Gleason grading 6. C–3: Gleason grading 7. C–4: Gleason grading 8. C–5: Gleason grading 9. C–6: Gleason grading 10. Original magnification 20×. Scale bars = 100 μm.

cells transfected with a scrambled siRNA (Fig. 5B). Similar results were seen using the C4-2B and LNCaP cell lines (not presented). Next, to explore the in vivo role of Anxa2r in PCa metastases, PC-3^{siAnxa2r} or PC-3^{siControl} cells were injected *i.c.* into SCID mice. At 1 month, significantly fewer lesions were identified in the PC-3^{siAnxa2r} cells injected group compared to those animals that received the cells expressing the scrambled controls (Fig. 5C). These data support the hypothesis that Anxa2r plays a critical role in PCa metastasis.

Anxa2 REGULATES PCa PROLIFERATION AND SURVIVAL VIA MAPK SIGNALING PATHWAY

To determine whether Anxa2 supports PCa survival or proliferation, we examined the viability of PC-3^{Luc} cells that were plated on osteoblasts derived from *Anxa2$^{+/+}$* or *Anxa2$^{-/-}$* mice. Significantly more PC-3^{Luc} cells grew on the *Anxa2$^{+/+}$* osteoblasts than on the *Anxa2$^{-/-}$* osteoblasts (Fig. 6A-1,2). To further explore whether Anxa2 supports PCa growth in vivo, PC-3^{Luc} cells were injected directly into vertebral bodies (vossicles) derived from *Anxa2$^{+/+}$* or *Anxa2$^{-/-}$* animals, and transplanted into immunodeficient hosts. Bioluminescent imaging was performed at one month to evaluate luciferase activity in the implanted vossicles. The data demonstrated that the growth of the PCa was greater in the vossicles derived from *Anxa2$^{+/+}$* animals (Fig. 6B-1,2). To explore how Anxa2 regulates survival/growth, we next examined the effects of Anxa2 on Erk1/2 or Akt activation in PCa cells. PCa cells were treated with Anxa2, and Akt and Erk1/2 phosphorylation were evaluated by western blotting. The data demonstrated that Anxa2 rapidly induces Erk1/2 phosphorylation in PC-3 cells within 5 min, whereas Anxa2 did not
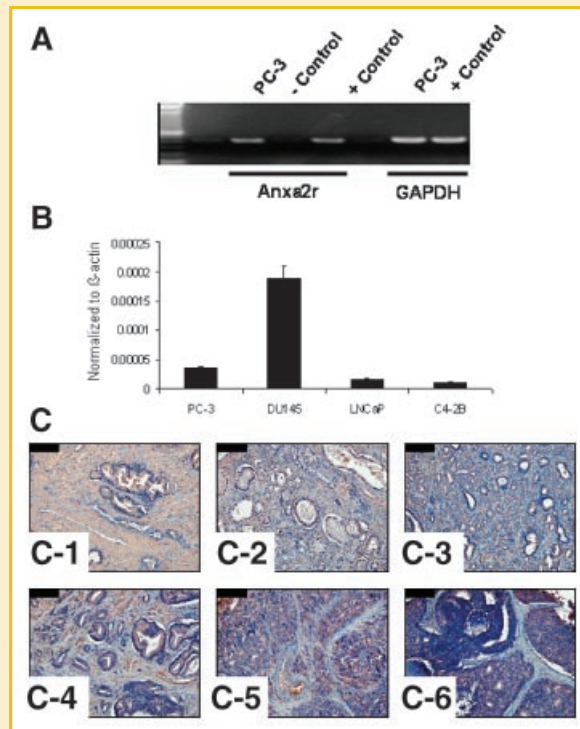
activate the Akt pathway (Fig. 6C). These data suggested that once PCa has metastasized to the bone, Anxa2 then facilitates the PCa growth via the MAPK pathway.

DISCUSSION

In this paper, we demonstrate that the Anxa2/Anxa2r axis plays a crucial role in establishing metastasis of PCa by regulating the adhesion and migration of PCa to osteobalsts and endothelial cells. PCa cells migrate toward Anxa2 and the adhesion of PCa to osteoblasts and endothelial cells was inhibited by an Anxa2 peptide, and an anti-Anxa2 antibody and by siRNA knockdown of Anxa2r. In in vivo studies, the short-term localization of PCa cells to a number of tissues was substantially inhibited by Anxa2 peptides or anti-Anxa2 antibodies. The long-term localization of PCa cells to a number of tissues was also inhibited by siRNA knockdown of Anxa2r. Moreover, Anxa2 is involved in the regulation of PCa growth in vitro and in vivo by activating the MAPK signaling pathway. Together, these data strongly suggested that Anxa2/Anxa2r axis plays an important role in regulating the metastasis of PCa to the marrow.
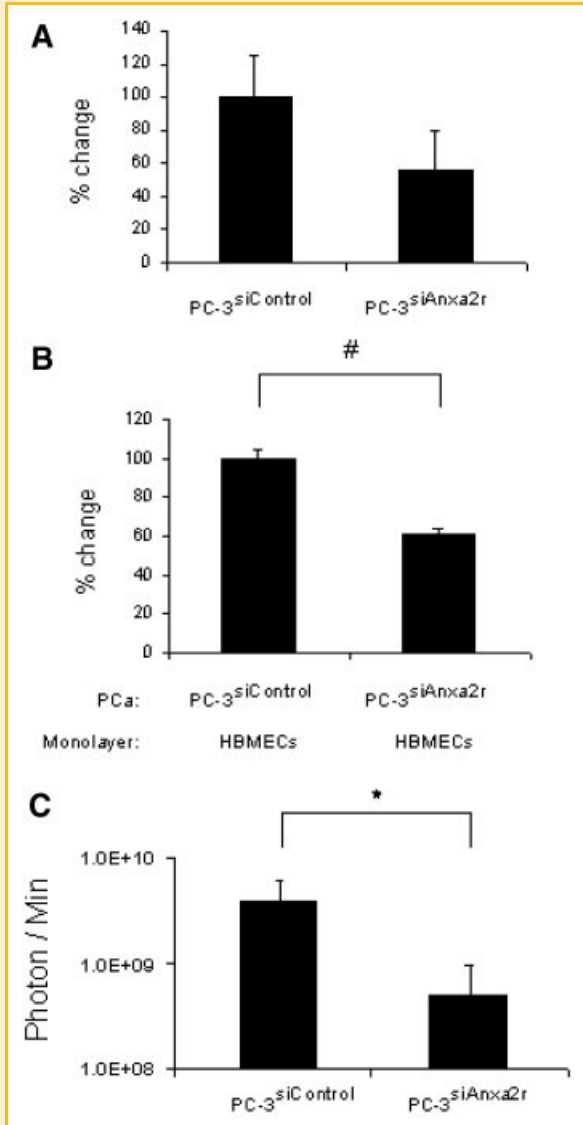
Fig. 5. Anxa2r–targeting siRNAs specifically inhibit adhesion of prostate cancer to endothelial cells in vitro, and tumor growth in vivo. PC-3^{Luc} cells were transfected with Anxa2r–targeting siRNAs (PC-3^{siAnxa2r} cells) or scramble control vector (PC-3^{siControl} cells). A: The expression of Anxa2r was evaluated by *Q*PCR at 48 h after transfection. β-actin was included as a loading control. B: Attachment of fluorescently labeled PC-3^{siAnxa2r} or PC-3^{siControl} cells to human bone marrow endothelial cells (HBMECs) at 4°C for 15 min. C: PC-3^{siAnxa2r} or PC-3^{siControl} cells were injected systemically by intracardiac injection into SCID mice. After a month, tumor growth was measured by a bioluminescent imaging. Bioluminescence images are presented as the relative photon counts of each individual (n = 10). Data are presented as the mean ± standard error. *$P < 0.05$ and #$P < 0.01$ versus control.

It is well known that HSCs localize to bone during fetal life and during marrow transplantation. In the bone marrow, HSCs are known to associate with at least 2 separate niches, the endosteal niche (osteoblasts) and the vascular niche (endothelial cells). We have recently demonstrated that osteoblasts and marrow endothelial cells express Anxa2 which functions as a molecule that regulates hematopoietic stem engraftment [Jung et al., 2007]. We have hypothesized based upon the hematopoietic model that metastatic

PCa use a similar pathway to localize to the bone marrow [Taichman et al., 2002]. Although both hematopoietic cells and PCa cells home to the bone marrow, we are not aware of any investigation that addresses whether Anxa2 operates in the pathogenesis of PCa metastasis as an adhesion ligand. Our functional studies demonstrate that Anxa2 alters the adherence, migration, and invasion of human PCa cell lines. For example, it was observed that PCa cells adhere to Anxa2 and that the N-terminal Anxa2 peptide dramatically inhibited PCa binding to bone marrow-derived endothelial cells. Moreover, it was demonstrated that Anxa2 supported the invasion of PCa cell lines into reconstituted extracellular matrices, and that invasion stimulated by CXCL12 could be blocked by with Anxa2 itself or the N-terminal Anxa2 peptide. In fact, recently we observed that CXCL12 binds to Anxa2, which could account for the loss of growth of PCa in $Anxa2^{-/-}$ vossicles and why the addition of Anxa2 to the migration chambers prevented chemotaxis to CXCL12 (Russell S. Taichman, unpublished work). While specific transendothelial migration assays were not performed, the initial binding of PCa cells to the endothelium is a necessary prerequesite for egress of tumors out of the vascular system. It was also demonstrated Anxa2 plays an important role in regulating the binding between PCa and osteoblasts. To further confirm the involvement of Anxa2 in the PCa metastasis, it was found that blocking Anxa2 with a monoclonal antibody or N-terminal peptide prevented PCa homing to the marrow and other sites of PCa metastasis. Collectively, our results suggest that PCa cells use Anxa2 as they spread to bone and other tissues.

Our data also suggest that Anxa2 may also regulate the proliferation of PCa cells at metastatic sites. Moreover, ligand binding of PCa cells to Anxa2 resulted in activation of Erk1/2 signaling. In bone, Anxa2 has been demonstrated to play a role in osteoclastic activation and osteoblast mineralization, although the mechanism for these actions remains unclear [Takahashi et al., 1994; Wang and Kirsch, 2002]. One scenario is that extracellular Anxa2 levels are regulated by 1,25-dihydroxyvitamin D3 that stimulates the proliferation of osteoclastic precursors possibly through T-cell intermediaries through the secretion of GM-CSF [Menaa et al., 1999]. Osteoclastic activity is critical for PCa growth in bone [Zhang et al., 2001]. Alternatively, Anxa2 may regulate vascular in growth that is critical for tumor proliferation. Although the detailed mechanisms for this remain unclear, Anxa2 may be involved in the survival or growth of PCa either in a direct or indirect way.

Work by our group and others have defined the role that CXCL12 and its receptors (CXCR4 and RDC1/CXCR7) play in the metastatic process of PCa [Taichman et al., 2002; Sun et al., 2003, 2005, 2007; Cooper et al., 2004; Wang et al., 2005, 2008; Havens et al., 2006]. In PCa, we observed that CXCR4 expression relates to increasing tumor grade [Sun et al., 2003] and that CXCL12 signaling through CXCR4 triggers the adhesion of PCa to bone marrow endothelial cells, by activating CD164 [Havens et al., 2006] and $\alpha_v\beta_3$integrins [Sun et al., 2007]. Moreover, a positive correlation exists between tissue levels of CXCL12 and sites where metastatic PCa lesions are observed suggesting a selective effect (pelvis, tibia, femur, liver, and adrenals) [Sun et al., 2005]. Interestingly we found a significant number of PCa cells in the prostate 24 h after *i.c.* injection. Previously we noted
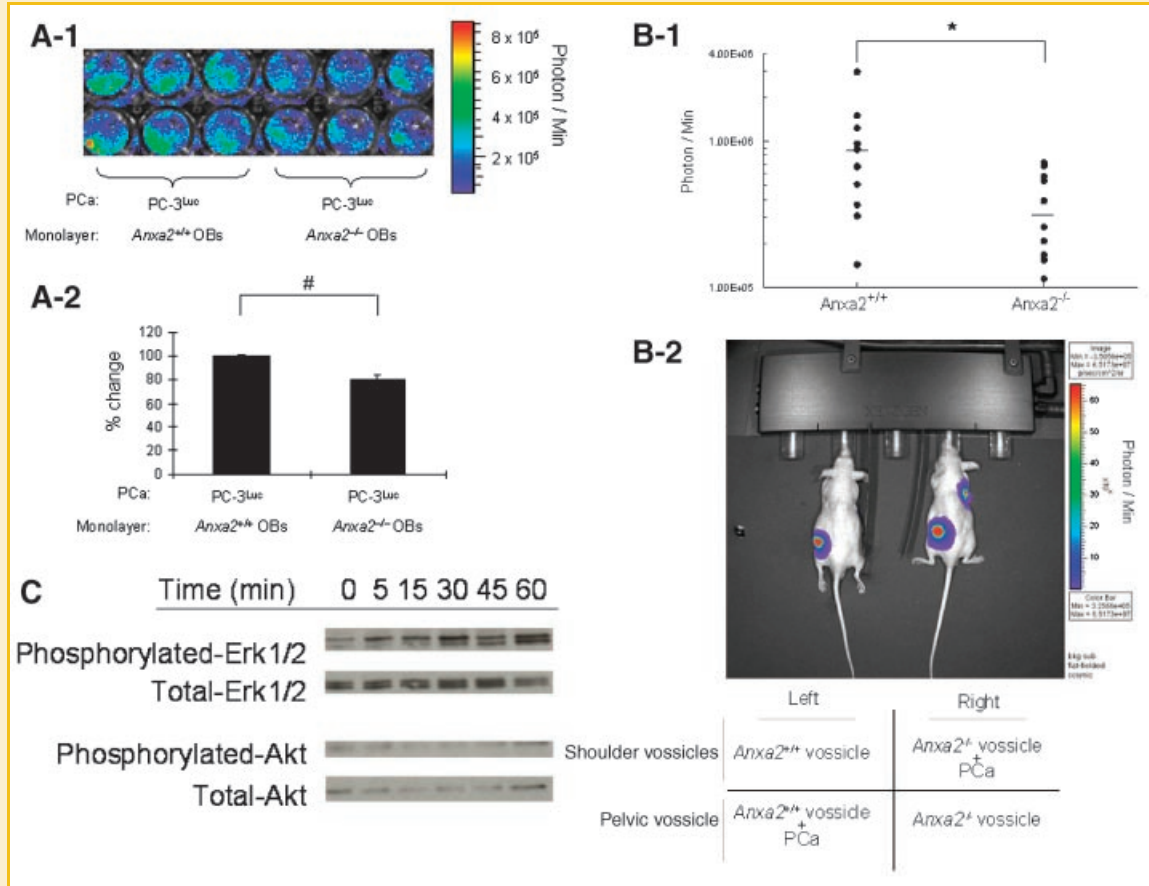
Fig. 6. Anxa2 facilitates the growth of prostate cancer in vitro and in vivo. A–1: The wild–type (*Anxa2*$^{+/+}$ OBs) or *Anxa2*$^{-/-}$ mouse osteoblasts (*Anxa2*$^{-/-}$ OBs) (10,000 cells/well) were plated onto 96-well plates with 0.1% FBS. The next day, PC-3^{Luc} cells (5,000 cells/well) were added on monolayers. At 72 h incubation at 37°C, luciferase activity was measured by a bioluminescent imaging. A–2: The graph shows the percent change of luciferase activity shown in (A–1) (n = 6). Data are presented as the mean ± standard error. $^{#}P < 0.01$ versus control. B–1: Growth of PC3 cells in an Anxa2 deficient osseous environment. PC-3^{Luc} cells were injected into *Anxa2*$^{+/+}$ and *Anxa2*$^{-/-}$ mice vossicles and transplanted into SCID mice (n = 12). At a month, the animals were imaged by a bioluminescent imaging. Data are presented as the relative photon counts of each individual. $^{*}P < 0.05$ versus control. B–2: Representative mice shown in (B–1). Individual animals were implanted with vossicles derived from either wild–type (*Anxa2*$^{+/+}$) or Anxa2 deficient animals. In some cases, these were seeded with PC3^{luc} cells as shown in animal map. C: PC-3 cells were cultured in medium without FBS for 5 h. After serum starvation, the cells were treated with 1,000 ng/ml Anxa2 peptide for 5, 15, 30, 45, and 60 min. Total protein was extracted and analyzed by Western blot for phosphorylated–Erk1/2 and Akt. Total Erk1/2 and Akt were used as an internal control for loading.

that PCa cells do disseminate back to the prostate from a *s.c.* tumor [Havens et al., 2008]. The basis for these observations however remains unclear. One of the mechanisms for this could be that prostate tissue expresses CXCL12 [Berquin et al., 2005]. Another could be that PCa cells are attracted to the primary site possibly due to other homing mechanisms or because of its "fertile soil." Further studies will be needed to sort out these possibilities.

While CXCL12 and its receptors participate in the homing of PCa to the niche, the events activated by PCa to co-opt the niche remain unclear. It is tantalizing to hypothesize that one of the potential reasons why metastatic PCa induce the expression of an osteoblastic phenotype is to establish a paracrine loop to further support their expansion/growth through enhanced production of CXCL12 and Anxa2. For example, Anxa2 itself is associated with proliferating and invasive cancers, possibly as a marker of malignancy [Reeves et al., 1992] including lung, pancreatic, brain, colon, and gastric carcinomas, and is correlated with poor prognosis [Cole et al., 1992;

Vishwanatha et al., 1993; Roseman et al., 1994; Emoto et al., 2001; Diaz et al., 2004]. Yet, the loss of Anxa2 expression appears to be specific for PCa disease [Chetcuti et al., 2001; Banerjee et al., 2003; Kirshner et al., 2003; Liu et al., 2003; Smitherman et al., 2004; Semov et al., 2005]. Therefore, it is possible that the absence of Anxa2 places selective pressures on PCa tumors to metastasize to bone, a rich source of Anxa2.

It is also possible that Anxa2 serves as an adhesion molecule for PCa such that blocking Anxa2 or its receptor limits metastasis and subsequent tumor growth. Part of the mechanism may be that engagement of Anxa2 receptors on PCa stimulates the expression of a number of other receptors on PCa, many of which may be activated by proliferative signals including CXCR4. Thus, a "vicious cycle" would be established by PCa in which increases in osteoblast numbers expand niche size by increasing the availability of Anxa2 and CXCL12. As a result, tumor expansion in the marrow may result by providing a docking signal that is normally absent (i.e., Anxa2)

and promotion of proliferation (i.e., CXCL12), which may explain why bone metastases are so difficult to treat clinically. While further studies are clearly needed, these data suggest that Anxa2/Anxa2r plays a significant role in the metastatic cascades of PCa and thereby suggest novel targets for therapeutic intervention to prevent PCa metastasis.

ACKNOWLEDGMENTS

REFERENCES

Arai F, Hirao A, Ohmura M, Sato H, Matsuoka S, Takubo K, Ito K, Koh GY, Suda T. 2004. Tie2/angiopoietin-1 signaling regulates hematopoietic stem cell quiescence in the bone marrow niche. Cell 118:149–161.

Banerjee AG, Liu J, Yuan Y, Gopalakrishnan VK, Johansson SL, Dinda AK, Gupta NP, Trevino L, Vishwanatha JK. 2003. Expression of biomarkers modulating prostate cancer angiogenesis: Differential expression of annexin II in prostate carcinomas from India and USA. Mol Cancer 2:34.

Baran D, Quail J, Ray R, Honeyman T. 2000. Binding of 1 alpha,25-dihydroxyvitamin D-3 to annexin II: Effects of vitamin D metabolites and calcium. J Bone Miner Res 15:S329–S329.

Berquin IM, Min Y, Wu R, Wu H, Chen YQ. 2005. Expression signature of the mouse prostate. J Biol Chem 280:36442–36451.

Brownstein C, Falcone DJ, Jacovina A, Hajjar KA. 2001. A mediator of cell surface-specific plasmin generation. Ann NY Acad Sci 947:143–155; discussion 155–156.

Calvi LM, Adams GB, Weibrecht KW, Weber JM, Olson DP, Knight MC, Martin RP, Schipani E, Divieti P, Bringhurst FR, Milner LA, Kronenberg HM, Scadden DT. 2003. Osteoblastic cells regulate the haematopoietic stem cell niche. Nature 425:841–846.

Chetcuti A, Margan SH, Russell P, Mann S, Millar DS, Clark SJ, Rogers J, Handelsman DJ, Dong Q. 2001. Loss of annexin II heavy and light chains in prostate cancer and its precursors. Cancer Res 61:6331–6334.

Chung CY, Erickson HP. 1994. Cell surface annexin II is a high affinity receptor for the alternatively spliced segment of tenascin-C. J Cell Biol 126:539–548.

Cole SP, Pinkoski MJ, Bhardwaj G, Deeley RG. 1992. Elevated expression of annexin II (lipocortin II, p36) in a multidrug resistant small cell lung cancer cell line. Br J Cancer 65:498–502.

Coleman RE. 2006. Clinical features of metastatic bone disease and risk of skeletal morbidity. Clin Cancer Res 12:6243s–6249s.

Cooper CR, Sikes RA, Nicholson BE, Sun YX, Pienta KJ, Taichman RS. 2004. Cancer cells homing to bone: The significance of chemotaxis and cell adhesion. Cancer Treat Res 118:291–309.

Diaz VM, Hurtado M, Thomson TM, Reventos J, Paciucci R. 2004. Specific interaction of tissue-type plasminogen activator (t-PA) with annexin II on the membrane of pancreatic cancer cells activates plasminogen and promotes invasion in vitro. Gut 53:993–1000.

Emoto K, Yamada Y, Sawada H, Fujimoto H, Ueno M, Takayama T, Kamada K, Naito A, Hirao S, Nakajima Y. 2001. Annexin II overexpression correlates with stromal tenascin-C overexpression: A prognostic marker in colorectal carcinoma. Cancer 92:1419–1426.

Falcone DJ, Borth W, Khan KM, Hajjar KA. 2001. Plasminogen-mediated matrix invasion and degradation by macrophages is dependent on surface expression of annexin II. Blood 97:777–784.

Fitzpatrick SL, Kassam G, Manro A, Braat CE, Louie P, Waisman DM. 2000. Fucoidan-dependent conformational changes in annexin II tetramer. Biochemistry 39:2140–2148.

Gerke V, Weber K. 1984. Identity of p36K phosphorylated upon Rous sarcoma virus transformation with a protein purified from brush borders; calcium-dependent binding to non-erythroid spectrin and F-actin. EMBO J 3:227–233.

Glenney JR Jr. 1986. Co-precipitation of intestinal p36 with a 73-K protein and a high molecular weight factor. Exp Cell Res 162:183–190.

Havens AM, Jung Y, Sun YX, Wang J, Shah RB, Buhring HJ, Pienta KJ, Taichman RS. 2006. The role of sialomucin CD164 (MGC-24v or endolyn) in prostate cancer metastasis. BMC Cancer 6:195.

Havens AM, Pedersen EA, Shiozawa Y, Ying C, Jung Y, Sun Y, Neeley C, Wang J, Mehra R, Keller ET, McCauley LK, Loberg RD, Pienta KJ, Taichman RS. 2008. An in vivo mouse model for human prostate cancer metastasis. Neoplasia 10:371–380.

Jung Y, Wang J, Song J, Shiozawa Y, Havens A, Wang Z, Sun YX, Emerson SG, Krebsbach PH, Taichman RS. 2007. Annexin II expressed by osteoblasts and endothelial cells regulates stem cell adhesion, homing, and engraftment following transplantation. Blood 110:82–90.

Kiel MJ, Yilmaz OH, Iwashita T, Terhorst C, Morrison SJ. 2005. SLAM family receptors distinguish hematopoietic stem and progenitor cells and reveal endothelial niches for stem cells. Cell 121:1109–1121.

Kirshner J, Chen CJ, Liu P, Huang J, Shively JE. 2003. CEACAM1-4S, a cell-cell adhesion molecule, mediates apoptosis and reverts mammary carcinoma cells to a normal morphogenic phenotype in a 3D culture. Proc Natl Acad Sci USA 100:521–526.

Koh AJ, Demiralp B, Neiva KG, Hooten J, Nohutcu RM, Shim H, Datta NS, Taichman RS, McCauley LK. 2005. Cells of the osteoclast lineage as mediators of the anabolic actions of parathyroid hormone in bone. Endocrinology 146:4584–4596.

Lehr JE, Pienta KJ. 1998. Preferential adhesion of prostate cancer cells to a human bone marrow endothelial cell line. J Natl Cancer Inst 90:118–123.

Liu JW, Shen JJ, Tanzillo-Swarts A, Bhatia B, Maldonado CM, Person MD, Lau SS, Tang DG. 2003. Annexin II expression is reduced or lost in prostate cancer cells and its re-expression inhibits prostate cancer cell migration. Oncogene 22:1475–1485.

Loberg RD, Day LL, Dunn R, Kalikin LM, Pienta KJ. 2006. Inhibition of decay-accelerating factor (CD55) attenuates prostate cancer growth and survival in vivo. Neoplasia 8:69–78.

Loberg RD, Ying C, Craig M, Day LL, Sargent E, Neeley C, Wojno K, Snyder LA, Yan L, Pienta KJ. 2007. Targeting CCL2 with systemic delivery of neutralizing antibodies induces prostate cancer tumor regression in vivo. Cancer Res 67:9417–9424.

Lu G, Maeda H, Reddy SV, Kurihara N, Leach R, Anderson JL, Roodman GD. 2006. Cloning and characterization of the annexin II receptor on human marrow stromal cells. J Biol Chem 281:30542–30550.

Mai J, Waisman DM, Sloane BF. 2000. Cell surface complex of cathepsin B/annexin II tetramer in malignant progression. Biochim Biophys Acta 1477:215–230.

Menaa C, Devlin RD, Reddy SV, Gazitt Y, Choi SJ, Roodman GD. 1999. Annexin II increases osteoclast formation by stimulating the proliferation of osteoclast precursors in human marrow cultures. J Clin Invest 103:1605–1613.

Menell JS, Cesarman GM, Jacovina AT, McLaughlin MA, Lev EA, Hajjar KA. 1999. Annexin II and bleeding in acute promyelocytic leukemia. N Engl J Med 340:994–1004.

Raynal P, Pollard HB. 1994. Annexins: The problem of assessing the biological role for a gene family of multifunctional calcium- and phospholipid-binding proteins. Biochim Biophys Acta 1197:63–93.

Reeves SA, Chavez-Kappel C, Davis R, Rosenblum M, Israel MA. 1992. Developmental regulation of annexin II (Lipocortin 2) in human brain and expression in high grade glioma. Cancer Res 52:6871–6876.

Roseman BJ, Bollen A, Hsu J, Lamborn K, Israel MA. 1994. Annexin II marks astrocytic brain tumors of high histologic grade. Oncol Res 6:561–567.

Semov A, Moreno MJ, Onichtchenko A, Abulrob A, Ball M, Ekiel I, Pietrzynski G, Stanimirovic D, Alakhov V. 2005. Metastasis-associated protein S100A4 induces angiogenesis through interaction with Annexin II and accelerated plasmin formation. J Biol Chem 280:20833–20841.

Smitherman AB, Mohler JL, Maygarden SJ, Ornstein DK. 2004. Expression of annexin I, II and VII proteins in androgen stimulated and recurrent prostate cancer. J Urol 171:916–920.

Sun YX, Wang J, Shelburne CE, Lopatin DE, Chinnaiyan AM, Rubin MA, Pienta KJ, Taichman RS. 2003. Expression of CXCR4 and CXCL12 (SDF-1) in human prostate cancers (PCa) in vivo. J Cell Biochem 89:462–473.

Sun YX, Schneider A, Jung Y, Wang J, Dai J, Cook K, Osman NI, Koh-Paige AJ, Shim H, Pienta KJ, Keller ET, McCauley LK, Taichman RS. 2005. Skeletal localization and neutralization of the SDF-1(CXCL12)/CXCR4 axis blocks prostate cancer metastasis and growth in osseous sites in vivo. J Bone Miner Res 20:318–329.

Sun YX, Fang M, Wang J, Cooper CR, Pienta KJ, Taichman RS. 2007. Expression and activation of alpha v beta 3 integrins by SDF-1/CXC12 increases the aggressiveness of prostate cancer cells. Prostate 67:61–73.

Taichman RS. 2005. Blood and bone: Two tissues whose fates are intertwined to create the hematopoietic stem-cell niche. Blood 105:2631–2639.

Taichman RS, Emerson SG. 1994. Human osteoblasts support hematopoiesis through the production of granulocyte colony-stimulating factor. J Exp Med 179:1677–1682.

Taichman RS, Cooper C, Keller ET, Pienta KJ, Taichman NS, McCauley LK. 2002. Use of the stromal cell-derived factor-1/CXCR4 pathway in prostate cancer metastasis to bone. Cancer Res 62:1832–1837.

Takahashi S, Reddy SV, Chirgwin JM, Devlin R, Haipek C, Anderson J, Roodman GD. 1994. Cloning and identification of annexin II as an autocrine/paracrine factor that increases osteoclast formation and bone resorption. J Biol Chem 269:28696–28701.

Thiel C, Osborn M, Gerke V. 1992. The tight association of the tyrosine kinase substrate annexin II with the submembranous cytoskeleton depends on intact p11- and Ca(2+)-binding sites. J Cell Sci 103(Pt 3):733–742.

Vishwanatha JK, Chiang Y, Kumble KD, Hollingsworth MA, Pour PM. 1993. Enhanced expression of annexin II in human pancreatic carcinoma cells and primary pancreatic cancers. Carcinogenesis 14:2575–2579.

Wang W, Kirsch T. 2002. Retinoic acid stimulates annexin-mediated growth plate chondrocyte mineralization. J Cell Biol 157:1061–1069.

Wang J, Sun Y, Song W, Nor JE, Wang CY, Taichman RS. 2005. Diverse signaling pathways through the SDF-1/CXCR4 chemokine axis in prostate cancer cell lines leads to altered patterns of cytokine secretion and angiogenesis. Cell Signal 17:1578–1592.

Wang J, Shiozawa Y, Wang Y, Jung Y, Pienta KJ, Mehra R, Lober R, Taichman RS. 2008. The role of CXCR7/RDC1 as a chemokine receptor for CXCL12/SDF-1 in prostate cancer. J Biol Chem 283:4283–4294.

Wu TT, Sikes RA, Cui Q, Thalmann GN, Kao C, Murphy CF, Yang H, Zhau HE, Balian G, Chung LW. 1998. Establishing human prostate cancer cell xenografts in bone: Induction of osteoblastic reaction by prostate-specific antigen-producing tumors in athymic and SCID/bg mice using LNCaP and lineage-derived metastatic sublines. Int J Cancer 77:887–894.

Zhang J, Dai J, Qi Y, Lin DL, Smith P, Strayhorn C, Mizokami A, Fu Z, Westman J, Keller ET. 2001. Osteoprotegerin inhibits prostate cancer-induced osteoclastogenesis and prevents prostate tumor growth in the bone. J Clin Invest 107:1235–1244.

Zhang J, Niu C, Ye L, Huang H, He X, Tong WG, Ross J, Haug J, Johnson T, Feng JQ, Harris S, Wiedemann LM, Mishina Y, Li L. 2003. Identification of the haematopoietic stem cell niche and control of the niche size. Nature 425:836–841.

Zhao WQ, Chen GH, Chen H, Pascale A, Ravindranath L, Quon MJ, Alkon DL. 2003. Secretion of Annexin II via activation of insulin receptor and insulin-like growth factor receptor. J Biol Chem 278:4205–4215.